European Journal of Pharmaceutical Sciences 191 (2023) 106600

Contents lists available at ScienceDirect

European Journal of Pharmaceutical Sciences

journal homepage: www.elsevier.com/locate/ejps

A comparison study between doxorubicin and curcumin co-administration and co-loading in a smart niosomal formulation for MCF-7 breast cancer therapy

Shaghayegh Saharkhiz [a], Atefeh Zarepour [b], Negar Nasri [a], Marco Cordani [c,d,*], Ali Zarrabi [b,*]

[a] Department of Biotechnology, Faculty of Biological Science and Technology, University of Isfahan, Isfahan, Iran
[b] Department of Biomedical Engineering, Faculty of Engineering and Natural Sciences, Istinye University, Istanbul 34396, Turkiye
[c] Department of Biochemistry and Molecular Biology, Faculty of Biological Sciences, Complutense University of Madrid, Madrid 28040, Spain
[d] Instituto de Investigaciones Sanitarias San Carlos (IdISSC), Madrid 28040, Spain

ARTICLE INFO

Keywords:
pH-responsive
Co-administration
Doxorubicin
Niosome
Cancer therapy

ABSTRACT

Chemotherapy agents often exhibit limited effectiveness due to their fast elimination from the body and non-targeted delivery. Emerging nanomaterials as drug delivery carriers open new expectancy to overcome these limitations in current chemotherapeutic treatments. In this study, we introduce and evaluate a smart pH-responsive niosomal formulation capable of delivering Doxorubicin (DOX) and Curcumin (CUR) in both individually and co-loaded forms. In particular, drug-loaded niosomes were prepared using thin-film hydration method and then characterized via different physicochemical analyses. The pH responsivity of the carrier was assessed by performing a drug release study in three different pH conditions (4, 6.5, and 7.4). Finally, the anticancer efficacy of the therapeutic compounds was evaluated through the MTT assay. Our results showed spherical particles with a size of about 200 nm and -2 mV surface charge. Encapsulation efficiency (EE%) of the nanocarrier was about 77.06 % and 79.08 % for DOX and CUR, respectively. The release study confirmed the pH responsivity of the carrier. The MTT assay results revealed about 39 % and 43 % of cell deaths after treatment with cur-loaded and dox-loaded niosomes, which increased to 74 % and 79 % after co-administration and co-loading forms of drugs, respectively, exhibiting increased anticancer efficacy by selectively delivering DOX and CUR individually or in combination. Overall, these findings suggest that our nanoformulation holds the potential as a targeted and highly effective approach for cancer management and therapy, overcoming the limitations of conventional chemotherapy drugs.

1. Introduction

Breast cancer is the most prevalent type of cancer among women accounting for approximately 12 % of newly diagnosed cancer cases, annually. A variety of several factors contribute to the formation and progression of this cancer, including inheritance, genetic mutation susceptibility, lifestyle habits, and patient personality traits (Fleege and Cobain, 2022). Currently, the primary treatment approaches for breast cancer are surgery, chemotherapy, and radiotherapy. To date, several drugs with different mechanisms of action have been developed for use in cancer chemotherapy. For instance, Doxorubicin (DOX) is a member of the anthracycline antibiotics family isolated from cultures of *Streptomyces peucetius var caesius* (Rawat et al., 2021). It exerts its effect by binding to the DNA double helix and inhibiting the formation of the DNA-Topoisomerase II complex during the cell division process (Elfadadny et al., 2023). Despite the remarkable anticancer activity of DOX, its conventional usage presents some limitations, such as a lack of specificity between healthy and cancerous cells, short half-lifetime in the circulation system, immunogenicity, and dangerous effects for healthy cells (Al-Malky et al., 2020).

Curcumin (CUR), also known as diferuloylmethane, is an herbal active component found in the golden spice turmeric (Curcuma longa) exhibiting antioxidant, antimicrobial, anti-inflammatory, anticancer, and wound-healing properties. However, its application is limited by factors such as poor water solubility, rapid metabolism, and swift systemic clearance (Gupta et al., 2013). In addition, previous reports have demonstrated a synergic therapeutic effect when DOX and CUR are co-administrated on Lymphoma cancer cells (Guo et al., 2020; Zhang

* Corresponding authors.
E-mail addresses: mcordani@ucm.es (M. Cordani), ali.zarrabi@istinye.edu.tr (A. Zarrabi).

https://doi.org/10.1016/j.ejps.2023.106600
Received 26 June 2023; Received in revised form 4 September 2023; Accepted 28 September 2023
Available online 5 October 2023

and Wu, 2022; Hong et al., 2019; Firouzi Amoodizaj et al., 2020).

Nanoparticles represent one of the most promising drug delivery systems (DDS) for addressing challenges related to the conventional administration of drugs, such as side effects, lack of treatment specificity, immunogenicity, low water solubility, and short half-life in blood (Meng et al., 2020). To date, several nanoparticles have developed as drug-delivery vehicles such as graphene oxide, silica, dendrimers, micelles, liposome, and noisome (Fatima et al., 2023). Liposomal and noisomal particles share a similar structure, composed of amphiphilic molecules that assemble in an aqueous medium and form a bilayer spherical structure. These nanoformulations have the potency to carry both hydrophilic and hydrophobic payloads. However, niosomes offer considerable advantages over liposomes including greater stability, lower cost, and ease of formulation and scaling up (Ge et al., 2019). Typical molecules incorporated into the niosome included non-ionic surfactants, cholesterol, and phospholipids. Non-ionic surfactants are the primary component of niosomes, while cholesterol provides additional stability, and reduces drug leakage. However, there is a limitation on the amounts of cholesterol that can be used, as incorporating more than 30 % cholesterol may decrease membrane flexibility and fluidity, impeding drug release (Ge et al., 2019; Nematollahi et al., 2017). An alternative approach for increasing particle stability, rather than relying solely on cholesterol, involves coating the particle surface with polyethylene glycol (PEG) molecules. PEG a highly biocompatible material, can be conjugated to the niosome surface via physical absorption or covalent bonding with surface functional groups of niosomes (Zarrintaj et al., 2020). This strategy increases the stability of particles, prolongs blood circulation time, and prevents their elimination from the body via the immune system (Zarrabi et al., 2021).

There are three strategies to improve the selectivity of DDSs: passive targeting, active targeting, and stimulus-responsive targeting. Stimulus-responsive targeting refers to the ability of DDSs to respond to specific features of the targeted tissue (Liu et al., 2016). For example, due to their enhanced metabolic activity, cancerous tissues exhibit a lower pH than healthy tissues, making the use of charge-reversible linkers such as citraconic anhydride (CA) an effective strategy for producing pH-responsive polymers (Lee and Shanti, 2021). The reaction between CA and an amine functional group forms a citraconic-amide bond that has a negative surface charge at neutral pH and a positive charge in acidic conditions due to bond cleavage (Saharkhiz et al., 2023). Based on our previous works, utilizing these polymers in combination with other noisomal components forms a stimulus-responsive stealth carrier for the targeted delivery of hydrophobic drugs including Curcumin in cancer chemotherapy (Zarrabi et al., 2021).

In previous work, our team formulated and evaluated new stealth pH-responsive niosomes for drug delivery and bio-imaging applications (Saharkhiz et al., 2023). Niosomes have also been investigated in other studies for the delivery of anti-inflammatory drug Naproxen and Sulfasalazine highlighting their potential as effective drug carriers (Erfani--Moghadam et al., 2020; Aghaei et al., 2021). Here, we employ this charge-reversible, pH-responsive carrier for the simultaneous delivery of hydrophilic Doxorubicin and hydrophobic Curcumin to the cancerous MCF-7 and normal L929 cell lines, comparing co-encapsulation and co-administration approaches. All the fabricated particles were characterized using different physiochemical analyses such as Dynamic Light Scattering (DLS), Zeta potential, Feriour Transmission Infera Red (FTIR) spectroscopy, and Scanning Electron Microscopy (SEM). Moreover, their drug loading capacity, drug release pattern, and cytotoxicity were assessed using different biological assays.

2. Materials and methods

2.1. Materials

1,2-distearoyl-sn-glycero-3-phosphocholine (DSPC, ≥ 99 %), 1,2-distearoyl-sn-glycero-3-phosphorylethanolamine (DSPE, ≥ 99 %), Sorbitan monostearate 60 (Span60, ≥ 99 %), polyoxyethylene-sorbitan-monostearate (Tween60, ≥ 99 %), cholesterol (Chol, ≥ 99 %), Dulbecco's modified Eagle's medium (DMEM) including 10 % fetal bovine serum (FBS), thiazolyl blue tetrazolium bromide (MTT) powder, and dimethylsulfoxide (DMSO), Dichloromethane (≥ 99.9 %), chloroform, diethyl ether (≥ 99.9 %), pyridine (99.8 %), and citraconic anhydride (CA, 98 %) were purchased from Sigma, Missouri, Midwestern State, USA. 2-propanol, ethanol, and dicyclohexylcarbodiimide (DCC) were bought from Merck, Darmstadt, Germany. Also, Trypsin-EDTA (0.5 %) and penicillin-streptomycin antibiotics were acquired from Thermofisher, Berman, Germany. Curcumin (≥ 99 %) and Doxorubicin hydrochloride (Dox HCl, ≥ 99 %) were purchased from Actore Co, Karaj, Iran. The chemicals were used without further purification. The MCF-7 and L929 cell lines also were acquired from the Pasteur Institute of Iran, Tehran, Iran.

2.2. Methods

2.2.1. Preparation of pH-responsive phospholipids

Initially, pH-responsive phospholipids were prepared according to our previous report (Saharkhiz et al., 2023). Briefly, 10 mmol pyridine, 10 mmol citraconic anhydride, and 2.5 mmol DSPE were dissolved in anhydrous dichloromethane (50 ml) and then stirred for approximately 30 min. Subsequently, 3.39 mmol of pre-dissolved DCC in 10 ml of dichloromethane were added to the mixture drop-wisely, and then the mixture was stirred for 24 h at room temperature, under an N_2 atmosphere. Next, 100 mg PEG2000 was added to the mixture and shacked for another 48 h at ambient temperature. Subsequently, the achieved solution was precipitated in 15 ml pre-cooled diethyl ether. The obtained DSPE-CA-PEG phospholipids were separated, redispersed in deionized (DI)-water (pH 7.4), and dialyzed against DI-water using a dialysis bag (molecular weight cut off 3.5 kDa) for 96 h and then lyophilized via a freeze dryer machine (VaCo 5, Zirbus, Bad Grund, Germany) (Zarrabi et al., 2021; Cao et al., 2014).

2.2.2. Fabrication of drug-loaded pH-responsive niosomes

To fabricate CUR and DOX co-loaded pH-responsive niosomes thin-film hydration method was used (Zarrintaj et al., 2020). For this purpose, 2 mg of CUR was dissolved in 10 ml of chloroform containing span60, tween60, cholesterol, and DSPC/DSPE-CA-PEG2000 with a 4.5: 1.5: 3: 0.5: 0.5 molar ratio, respectively, and stirred for 15 min. After that, the solvent was evaporated under a vacuum at 60 °C using a rotary evaporator (STEROGLASSsr1, STRIKE 202, Italy) to form a uniform yellow thin film. In the next step, 2 mg of DOX was added to 10 ml pre-heated phosphate-buffered saline solution (pH 7.4, 60 °C) and then added to the thin film and stirred for 1 h at 60 °C. Then, to reduce the size of the particles and form single-lamellar niosomes, the solution was sonicated for 1 h in an ice bath using a probe sonicator (Epishear, Japan). Finally, purification was done via dialysis method (24 h h, 12 kDa dialysis bag, against PBS). The single-drug-loaded niosomes were prepared with a similar procedure.

2.3. Characterization

2.3.1. Dynamic light scattering (DLS) and zeta potential analysis

To determine the size and surface charge of the fabricated pH-responsive niosomes with and without drugs, DLS and Zeta Potential analysis were employed, respectively. For this aim, the particles were dispersed in PBS solution and analyzed using a zeta sizer (HORIBA, Scientific SZ-100, Japan) at 25 °C.

2.3.2. Fourier-transform infrared spectroscopy (FTIR) analysis

To evaluate the correct fabrication of pH-responsive niosomes Fourier transform infrared (FTIR) spectroscopy (JASCO, FT/IR 6300, Japan) analysis was conducted in the range of 400 - 4000 cm^{-1} wavenumbers using KBr salt.

2.3.3. Scanning electron microscopy (SEM)

The size and morphology of the obtained DOX and CUR co-loaded particles were determined using a scanning electron microscope on the niosomal suspension (SEM, Leo, 1430 VP, Germany). Briefly, the suspension of samples was dropped on the grid, airdried, coated with an Au layer, and then evaluated via SEM.

2.4. Bio-activity assessments

2.4.1. In vitro entrapment efficiency (EE%) evaluation

To measure the amount of drugs loaded in the nanoparticles, 300 μl of drug-loaded niosomal suspension was mixed with 2700 μl of 2-propanol (1% w/v solution in water) and then agitated for approximately 48 h at room temperature to disrupt the particle structure (Haghiralsadat et al., 2018). Next, the mixture was centrifuged at 10,000 rpm to separate the niosomal fragments from the released drugs and the supernatants were analyzed using an LC-20AD HPLC system (Shimadzu, Japan) with an RF-10AXL fluorescence detector (Shimadzu, Japan). Separation was conducted on a Sepax Technologies Amethyst C18-H column (4.6 mm × 250 mm, 5 μm). The mobile phase consisted of methanol, 0.2 % trifluoroacetic acid (TFA) in water, and acetonitrile. Briefly, 40 μl of the supernatant was injected into the column for 20 min with a flow rate of 1 ml/min using the program detailed in Table 1. The absorbance of CUR was measured at 420 nm, and the DOX absorbance was determined at 250 nm and 485 nm. Then, the percentage of entrapment efficiency (EE%) was determined using the following equation (Eq. (1)) (Tian et al., 2018; Abouzeid et al., 2013; Sesarman et al., 2018):

$$\text{Entrapment Efficiency}\,(\%) = \text{Mass}\,(\text{Loaded drug})/\text{Mass}\,(\text{Total drug}) \times 100 \quad (1)$$

2.4.2. Evaluation of particles stability

To assess the long-term stability of the particles, their size, morphology, and EE % were determined after four months of storage at 4 °C.

2.4.3. Drug release pattern and release kinetic analysis

To determine the release profile, solutions of drug-loaded particles were placed in the dialysis bags (12 kDa cut-off) and immersed in phosphate-buffered saline (PBS) at three different pH levels (4, 6.5, and 7.4 that simulate the pH of the lysosome, cancer tissue, and normal tissue, respectively). The samples were then incubated at 37°°C. The amounts of released drugs were quantified by measuring the absorbance of the external solutions at 420 nm for CUR, and 485 and 250 nm for DOX at predetermined interval times (2, 4, 6, 12, 24, 48, 72, and 96 h h) using high-performance liquid chromatography (HPLC). Additionally, different mathematical models were applied to the data to determine the release kinetics of both drugs (Table 2) (Dash et al., 2010; Barzegar-Jalali, 2008).

2.4.4. MTT assay

The MTT colorimetric assay was conducted on MCF-7 cells (cancerous cell line) and L929 cells (normal cell line) to determine the cytotoxic effects of the synthesized particles (Aghaei et al., 2021). Briefly, 6×10^3 cells were seeded in each well of 96 well plates and incubated for 24 h at 37°°C and 5 % CO_2. Subsequently, the old media were replaced with fresh media containing two different concentrations (0.25 and 250 μg/ml) of various treatments, including free curcumin, free doxorubicin, CUR-loaded niosome, DOX-loaded niosome, and co-loaded niosomes. The CUR-loaded particles and DOX-loaded niosomes were co-administered with a ratio of 1:1 and then incubated for 24, 48, and 72 h h at 37 °C. After that, cells were washed twice with PBS and then 200 μl of fresh media containing 20 μl of MTT solution (5 mg/ml in PBS) was added to each well and incubated for 4 h at 37 °C. After that, the solution of each well was replaced with 200 μl DMSO and incubated for another 1 h in the dark at 37 °C and then the absorbance of each well was read at 570 nm via ELISA reader (Bio-Rad, Hercules, CA, USA).

Table 1
The utilized HPLC program of CUR and DOX separation.

Time (min)	Acetonitrile (v/v %)	Water with 0.2 % TFA(v/v %)	Methanol (v/v %)
0	25	50	25
7	25	50	25
8.5	40	40	20
10	60	30	10
11.5	80	20	0
13	100	0	0
16	100	0	0
17	25	50	25
20	25	50	25

Table 2
Different release kinetic model equations.

Number	Release kinetic model name	Equation
1	Zero-release kinetic model	$C = k_{0.}t$
2	First-release kinetic model	$LogC_0 - LogCt = kt/2.303$
3	Higuchi release kinetic model	$Log\ Q = log\ k_H + 1/2logt$
4	Hixson-Crowell release kinetic model	$Q_0^{1/3} - Q_t^{1/3} = k_{HC.}t$

(1). C= drug concentration, k_0 = rate constant of the zero-order model, t = time (2).C_0 = the drugs initial concentration, Ct = drug released amount in time t (3). Q = drug released amount in time t per unit area, k_H = Higuchi dissolution constant (4). Q_0 = drugs initial amount, Q_t = remained drug amount at time t, k_{HCt} = Hixson-Crowell rate constant (Chime et al., 2013).

2.4.5. Analysis of IC50 and combination index (CI)

The half maximal inhibitory concentration (IC50) value of different treatments was determined, as well. For this aim, 5×10^5 MCF-7 cells were cultured in each well of the 12-well plate and then treated with four different concentrations of each treatment (10^3, 10^4, 10^5, and 10^6 ng/ml) and incubated for 24 h h at 37 °C. Subsequently, the Combination Index (CI) value of the co-administration and co-loading of CUR and DOX was determined based on Chou and Talalay's method (Eq. (2)) to evaluate the interaction between the co-administered drugs.

$$CI = a/A + b/B \quad (2)$$

In this equation, 'A' denotes DOX IC50 in single-form usage at a concentration of 'a', and 'B' signifies the curcumin IC50 in an individual application form at a concentration of 'b'. According to this method, a CI value below 1, indicates a synergistic interaction between the two drugs, a value above 1 suggests an antagonistic interaction and a CI value of 1 implies an additive interaction between them (Chou et al., 1994; Foucquier and Guedj, 2015; Chou and Talalay, 1984).

2.5. Statical analysis

SPSS software (version 21, parametric analysis of variance, ANOVA (Tukey)) was employed to investigate the significance of quantitative data. Results were assessed based on the *P-value* ≤ 0.05.

3. Results

3.1. Preparation and characterization of DOX-loaded and CUR-loaded pH-responsive niosomes

3.1.1. DLS and zeta potential analysis

The size and surface charge of empty, DOX-loaded, CUR-loaded, and co-loaded pH-responsive niosomes were determined by DLS and Zeta potential (Table 3). The obtained results revealed 169.8 nm, 223.4 nm, and 273.1 nm in size for DOX-loaded, CUR-loaded, and co-loaded

Table 3
DLS and Zeta potential results of pH-responsive niosomes with different components.

Sample name	Size(nm) ± SD	PDI ± SD	Zeta potential (mv) ± SD
Empty niosomes	165.6 ± 1.2 nm	0.31 ± 0.01	−1.6 ± 0.04
DOX-loaded niosomes	169.8 ± 1.8 nm	0.34 ± 0.09	−1.7 ± 0.1
CUR-loaded niosomes	223.4 ± 2.3 nm	0.37 ± 0.05	−1.0 ± 0.05
Co-loaded niosomes	273.1 ± 3.1 nm	0.3 ± 0.02	−1.2 ± 0.08

particles, while the empty niosomes showed a size of about 165.6 nm. So, it seems that the entrapment of curcumin between the bilayer of the niosomes caused about a 50 nm increment in particle size while entrapping DOX in the core of niosomes didn't cause any significant change (Aibani et al., 2020). Moreover, nearly the same zeta potential for all samples confirmed the same structure for them as well as the absence of drug molecules on the surface of drug-loaded niosomes. Besides, a neutral surface charge confirmed the presence of PEG on the surface of niosomes (Zarrabi et al., 2021).

3.1.2. FTIR analysis

FTIR analysis was used to confirm the correct formation of the niosomes in different forms. Fig. 1-a showed the comparison between FTIR results of DOX-loaded niosomes, co-loaded niosomes, and empty niosomes. The obtained data showed three prominent peaks at approximately 793, 1573, and 1655 cm^{-1} corresponding to the C—H stretching bond of benzene, the C═C bond of ketone, and the C═O bond of carbonyl groups of doxorubicin, respectively (Saharkhiz et al., 2023; Aliman et al., 2021). Also, the O—H stretching bond at 3477 cm^{-1} was observed in the spectra of free doxorubicin, empty niosome, and DOX-loaded niosome, with higher intensities in the DOX-loaded samples and doxorubicin compared to the empty niosomes. These results corroborate the incorporation of doxorubicin within the niosomal structure, leading to enhancement in the O—H bond intensity in DOX-loaded particles in comparison with bare niosomes (Aliman et al., 2021). On the other hand, Fig. 1-b displays the FTIR spectrum of pure curcumin, curcumin-loaded, and co-loaded niosomes. The achieved data identified four peaks at approximately 1118, 1490, 1589, and 3473 cm^{-1} which were attributed to the C—O bending bond of ether, C—H bending bond of methylene, C═C stretching bond of ketone, and the O—H stretching bond of curcumin, respectively (Gunathilake et al., 2022). Moreover, the emergence of the C—O bond of Esther and the C—H bond of alkyl groups in all niosomal samples confirmed the presence of Tween 60 and Span 60 components in the structure of the niosomes (Saharkhiz et al., 2023; Javani et al., 2021). It is worth noticing that in both spectra an N—C stretching bond was seen at approximately 1620 cm^{-1}, confirming the presence of the DSPE-CA-PEG2000 polymers in the structure of the particles (Saharkhiz et al., 2023).

3.1.3. SEM analysis

To evaluate the morphology of the niosomes scanning electron microscopy was performed. As illustrated in Fig. 2, the particles have spherical shapes and smooth surfaces with an average size of around 100 nm with homogeneous size distribution. Basically, in comparison to our previous study, the co-loading of DOX and CUR did not affect the shape of the particles (Saharkhiz et al., 2023).

3.2. Bio-activity assessments

3.2.1. In vitro entrapment efficiency (EE%) assessments

The EE% measurement revealed approximately 80.1 % ± 1.4 for DOX-loaded particles and 88.3 % ± 0.2 for CUR-loaded niosomes. Furthermore, these values for co-loaded particles were about 77.76 % ± 4.2 and 79.08 % ± 0.9 for DOX and CUR, respectively. Based on these observations, we hypothesize that the co-loading of DOX and CUR did not affect the entrapment capacity of the particles.

3.2.2. Stability evaluation

SEM imaging and EE% measurements were conducted on preformed niosomal particles after four months to assess any alteration in shape, size, and their ability to retain their cargo. The SEM images revealed no significant change in size, although some particle aggregation was observed (Fig. 3). Additionally, the repeated EE% measurements showed a decrease of approximately 13 % and 5 % in the amount of entrapped CUR and DOX, respectively (Table 4). This adequate particle stability could be related to the presence of biocompatible PEG polymer in the structure of the niosome (Javani et al., 2021).

3.2.3. Drugs release pattern and kinetic release models

To determine the release pattern of hydrophilic DOX and hydrophobic CUR from pH-sensitive niosomes in response to pH variations, the particles were exposed to PBS with three different pH levels (4, 6.5, and 7.4) for 4 days (Fig. 4**a and b**). The DOX release results showed an initial burst phase in the first 12 h h, exhibiting greater drug release at more acidic pH levels. Specifically, at pH 4, approximately 45.45 % of DOX was released, while these values were 25.6 %, and 18.4 % for pH 6.5 and 7.4, respectively. This burst phase may be due to the release of entrapped DOX molecules from the PEG 2000 polymer branches and the movement of DOX molecules following the concentration gradient. Additionally, it appears that the amide bond between citraconic anhydride and DSPE was broken, and the CA-PEG 2000 layer was separated during this phase. Subsequently, DOX release occurred in a more controlled manner, while maintaining the pH sensitivity of particles, which can be attributed to the weak pH-responsive nature of the DSPE molecules (Cao et al., 2014; Ghaffari et al., 2020).

The CUR release results revealed a sustained drug release pattern with a slow rate during the initial 48 h h, with approximately 17.78 % and 25.59 % of the drugs being released at pH 7.4 and 6.5, respectively. This percentage increased significantly at pH 4, reaching approximately 79.08 % (Fig. 4**c and d)**. We hypothesize that the separation of the CA-PEG layer in response to the environmental acidity facilitated the enhanced CUR leakage from the niosomal bilayer to the external media. Remarkably, the amount of drug release increased when the pH of the medium changed to a more acidic pH. In subsequent hs, CUR release also followed a controlled pattern, providing a prolonged release which leads to fewer doses of medication need (Lookabaugh and Von Gunten, 2018). We hypothesize that the sustained release manner of CUR was due to their placement between the bilayer of the niosomes, releasing simultaneously with a slow rate. Moreover, it is important to note that no difference was observed in the drug release profile of DOX and CUR from single drug-loaded and co-loaded particles, proving the co-loading of two drugs does not interfere with the release of each other.

Mathematical calculations were performed to identify the kinetic release model of the samples, and their corresponding plots are presented in Table 3. The R^2 values indicate that the release patterns for both drugs fit the Higuchi kinetic release model (Table 5), which represents a consistent diffusion of drug molecules in one direction from the particles to the external environments (Dash et al., 2010).

3.2.4. MTT assay

The MTT assay was employed to evaluate the cytotoxicity of different concentrations of pH-responsive niosomes (Fig. 5) on MCF7 and L929 cells. Cells were treated with different concentrations of DOX-loaded, CUR-loaded, and co-loaded particles, as well as their co-administration, for 72 h h. Importantly, the empty pH-responsive niosomes exhibited negligible cytotoxicity on both MCF-7 and L929 cell lines, validating the biocompatibility of the synthesized nano-carriers. Moreover, for all drug-loaded niosome types, increasing the

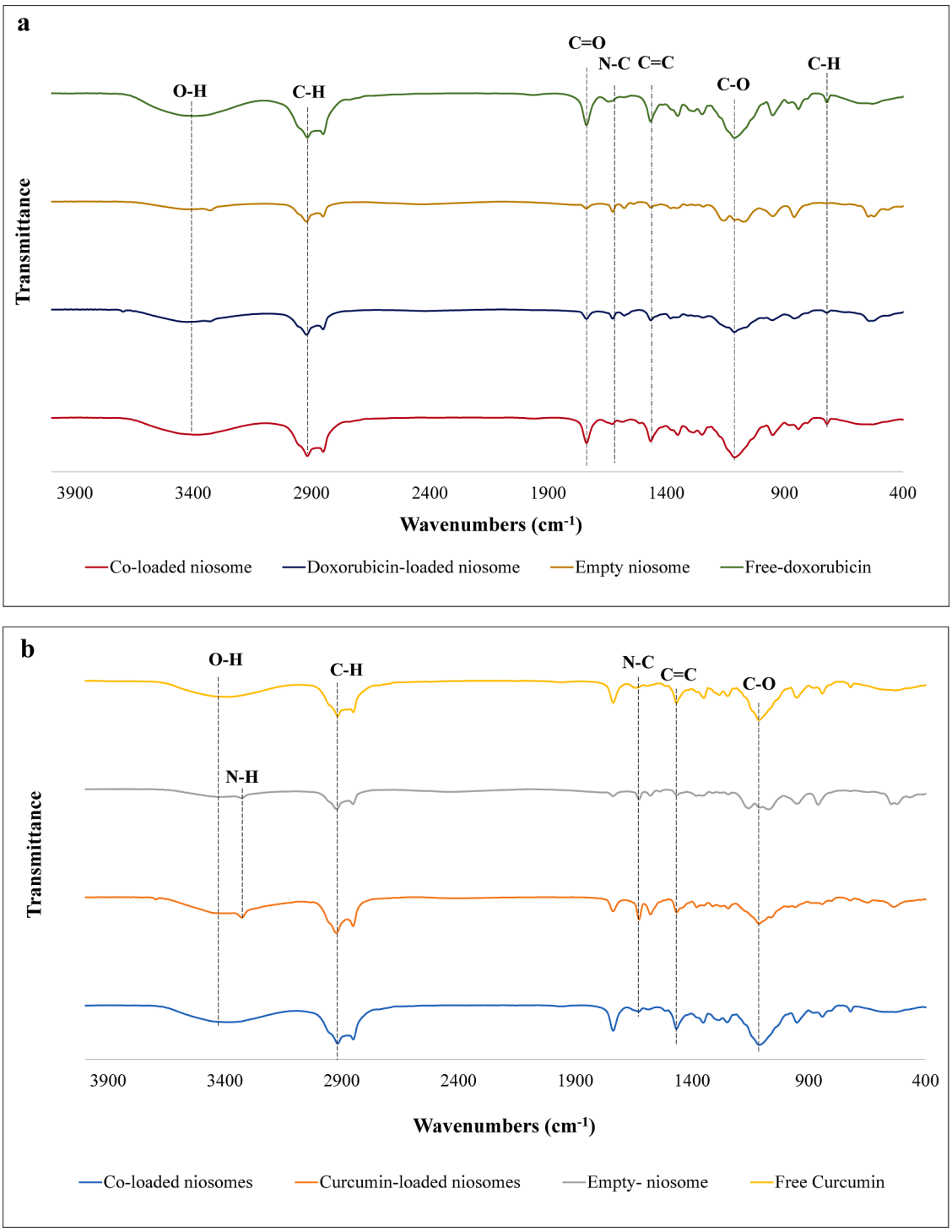

Fig. 1. (a) FTIR spectrum of free doxorubicin and DOX-loaded pH-responsive niosomes; (b) FTIR spectrum of pure curcumin and curcumin-loaded niosomal particles.

concentration enhanced the cytotoxicity effect on cancer cells, demonstrating a concentration-dependent response. Specifically, using 250 μg/ml of CUR-loaded and DOX-loaded particles resulted in a 20 % and 17 % higher cell death rate compared to 0.25 μg/ml, respectively. Notably, the co-administration of DOX-loaded and CUR-loaded particles exhibited a synergistic effect, substantially reducing MCF-7 cell viability from 61 % to 30 % after 72 h h of incubation. Similarly, co-loading of CUR and DOX caused a comparable reduction in cell viability for MCF7 breast cancer cells, from 57 % to 26 %, indicating no significant difference in cytotoxic activity between co-administration and co-loading of DOX and CUR within these pH-responsive niosomal particles. Meanwhile, normal cells L929 display minimal cytotoxic effects, further demonstrating the specificity of the treatment. Importantly, both strategies resulted in a synergistic effect on cancer cells while maintaining relatively low toxicity toward normal cells. All data were statically analyzed using SPSS, with a p-value of less than 0.05, confirming the significance of the observed results.

3.2.5. IC50s and CI values measurements

To assess the inhibitory effect of individual DOX and CUR, as well as

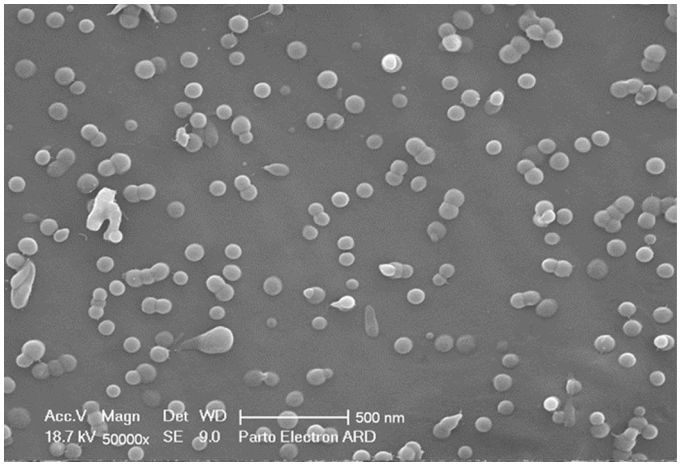

Fig. 2. SEM images of the drug-loaded pH-responsive niosomes at a 500 nm scale bar which present round-shaped particles.

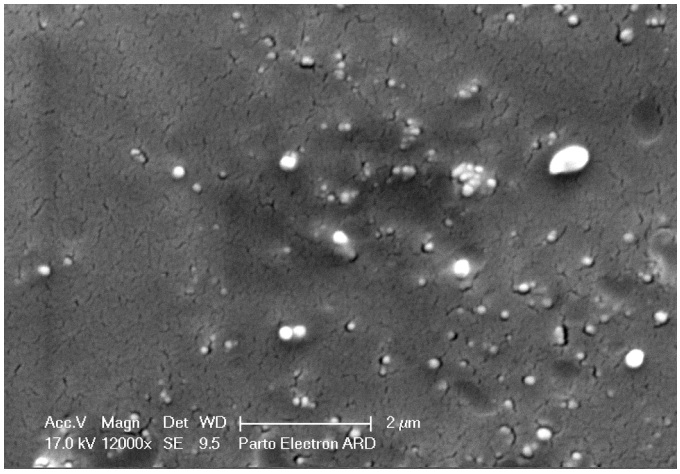

Fig. 3. SEM image of the co-loaded pH-responsive niosomes after 4 months of storage at 4 °C which represents no size change and a little aggregation.

Table 4
The results of DLS and EE% measurements of the single and co-drug loaded pH-responsive niosomal particles at $t = 0$ and $t = 4$ months.

Sample	Size (nm ± SD)	EE% ± SD (in $t = 0$)	EE% ± SD (in $t = 4$)
CUR-loaded niosomes	242.7 ± 1.8 nm	88.3 ± 0.2	85.1 ± 0.6
DOX-loaded niosome	191.9 ± 0.9 nm	80.1 ± 1.4	66.8 ± 2.6
Co-loaded niosome	298.6 ± 2.3 nm	77.76 ± 4.2 (DOX) 79.08 ± 0.9 (CUR)	62.01 ± 1.5 (DOX) 71.50 ± 0.7 (CUR)

their niosomal forms, on MCF-7 cells, dose-dependent experiments were performed (Fig. 6**a and b**), and the corresponding IC50 values were evaluated (Table 6). The results revealed that the IC50 values for free DOX and CUR were approximately 129.3 μg/ml and 138.7 μg/ml, respectively. Upon encapsulation within niosomes, these values increased to 231.2 μg/ml and 249.3 μg/ml, respectively. These findings indicate that CUR-loaded niosomes required ~ 1.78-fold higher concentrations, and DOX-loaded niosomes necessitated ~ 1.81-fold higher concentrations to reach IC50, compared to their respective free drugs (Table 6). Subsequently, the calculated IC50 values were used as fixed ratios to determine the combination index (CI) and evaluate the interaction between DOX and CUR in co-administration and co-loading scenarios (Table 7). For this aim, MCF-7 cancer cells were exposed to DOX-loaded, CUR-loaded, and co-loaded niosomes. Additionally, the cancer cells were exposed simultaneously to both individual DOX-loaded and CUR-loaded particles. The results showed that co-administration of CUR-loaded particles with DOX-loaded niosomes enhanced cell growth inhibition by approximately 3.9-folds while co-loaded particles increased this effect to ~ 4.4 folds. In addition, the calculated CI values for niosomal forms of DOX and CUR (Table 7) present values below 1, indicating a synergistic interaction between the two drugs for inhibiting cell growth in both co-loaded and co-administrated forms (Foucquier and Guedj, 2015).

4. Discussion

Recently, there has been growing interest in the use of herbal compounds with anti-cancer activity, such as curcumin. The simultaneous administration of these active compounds with chemotherapy agents is believed to enhance the therapeutic effect of both drugs compared to their individual use. Moreover, this strategy can potentially reduce the side effects of anti-cancer chemical drugs due to the lower required dosage (Dhillon et al., 2008; Shehzad et al., 2010). To leverage these advantages against MCF-7 cells, we selected doxorubicin, a chemotherapy agent, and curcumin, an active herbal compound, for simultaneous use. Despite the therapeutic benefits of co-administrating doxorubicin and curcumin in the treatment of various cancer types, challenges such as curcumin's poor solubility and doxorubicin's toxic side effects remain. Nanotechnology has provided solutions to overcome these obstacles, through the development of many nanocarriers designed to deliver these drugs individually or in combination. In 2015, Wang et al. co-encapsulated DOX and CUR in a polymeric micelle, performing *in vitro and in vivo* studies on their combination use. Interestingly, their *in vitro* results on the MCF-7 cell line, similar to our findings, demonstrated 40 % and 20 % increased toxicity for the combination use of DOX and CUR compared to their single use. Furthermore, *in vivo* experiments showed about 200 mg more tumor weight loss than single drug usage. It is worth noting that the drug release pattern of both drugs from their synthesized nano micelles was similar to our work, although with lower amounts of released drugs (Wang et al., 2015). Gau and co-workers also investigated polypeptide nanocarriers for simultaneous loading of DOX and CUR. Their observations revealed comparable release patterns of DOX and CUR to our fabricated carriers but with lower percentages of released drugs. Moreover, their cytotoxicity assessments confirmed the synergistic interaction of CUR and DOX co-administration for the treatment of cancer cells, consistent with our data (Guo et al., 2020). In another research done by Sesarman et al. in 2018, co-loading of curcumin and doxorubicin in a liposome comprising of Dipalmitoylphosphatidylcholine (DPPC), 1,2-Distearoyl-sn-glycero-3-phosphorylethanolamine (DSPE)-PEG2000, and Cholesterol resulted in a three-fold decrease in tumor weight compared to single drug-loaded liposomal forms (Sesarman et al., 2019).

The results of both studies align with our findings, which demonstrated that the combined use of two drugs reduced cell viability to approximately 20 % in both co-loaded niosomes and co-administration of DOX-loaded and CUR-loaded particles. In contrast, single drug-loaded samples reduced cell viability to about 58–65 percent after 72 h h of incubation with treatments. Among various nano-drug delivery carriers, vesicular nanocarriers such as liposomes and niosomes have gained considerable attention. These carriers have addressed several issues associated with the unprotected use of the drugs; however, challenges persist, including drug leakage during transport and the lack of specificity of these particles. Consequently, many strategies have been developed to overcome these limitations, including passive targeting, active targeting, and smart drug delivery approaches. Smart drug delivery refers to the specific release of drugs in a targeted area in response to extrinsic (*e.g.*, light or magnetic fields) or intrinsic (*e.g.*, pH or

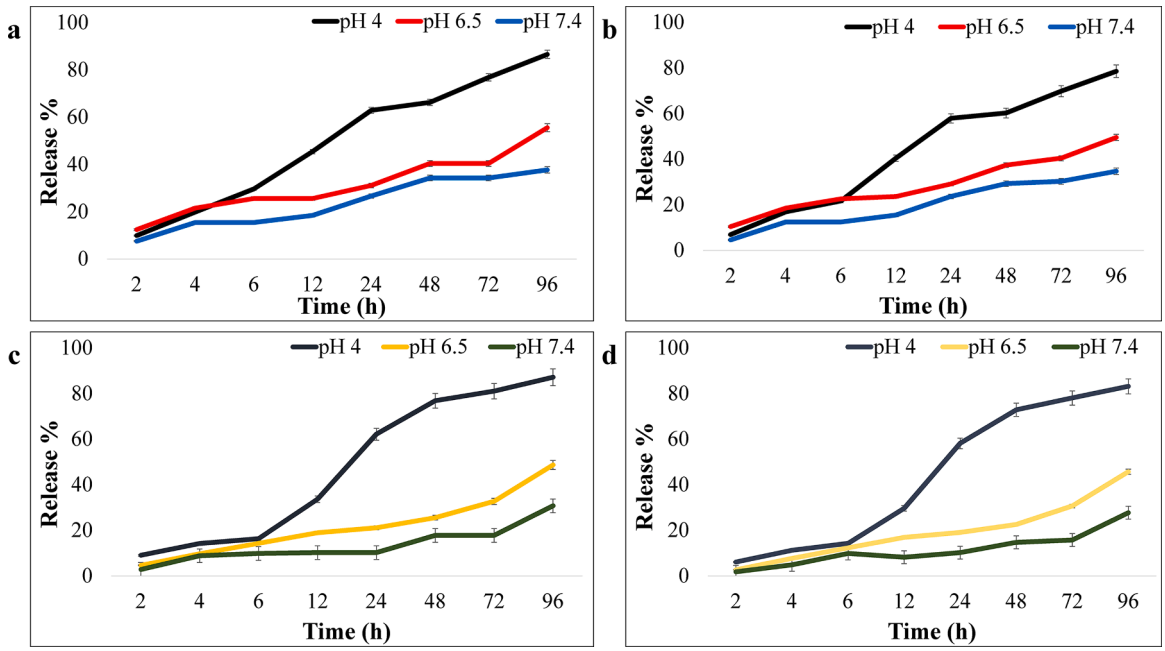

Fig. 4. (a) The release pattern of DOX from DOX-loaded pH-responsive niosome; (b) DOX release profile from co-loaded particles; (c) the release pattern of CUR from CUR-loaded niosomal particles; (d) CUR release behavior of co-loaded particles at different pH values: 4, 6.5 and 7.4.

Table 5
R^2 values of DOX and CUR release in different kinetic release models.

Kinetic release model name	R^2 value for DOX release			R^2 value for CUR release		
	pH 4	pH 6.5	pH 7.4	pH 4	pH 6.5	pH 7.4
Zero model	0.9698	0.9524	0.9418	0.9148	0.9704	0.8314
First model	0.9839	0.9436	0.9419	0.9564	0.9683	0.9157
Higuchi model	0.9866	0.9866	0.9866	0.9873	0.9873	0.9873
Hixson model	0.8249	0.8843	0.9215	0.7736	0.9792	0.91

temperature) stimuli (Liu et al., 2016). In this study, we exploited the slightly acidic pH of cancerous tissue (6.5–7) compared to normal tissue (7.4) and designed pH-responsive DSPE-CA-PEG2000 phospholipids, which were incorporated into the niosomal structure.

A number of studies have utilized various methods to harness smart drug delivery for targeting cancer cells. In this regard, in 2014, Cao and colleagues developed a novel pH-responsive polymer by attaching a citraconic anhydride molecule to methoxy poly(ethylene glycol)-b-poly (e-capro-lactone) copolymer via a citraconic-amide bond, functioning as a pH-sensitive bond, while PEG 2000 molecules were linked through an ester bond. The obtained polymers were self-assembled into micelle structures to deliver DOX molecules to HepG2 and 4T1 cancer cells. Their findings revealed that the fabricated micelles exhibited a pH-responsive drug-release pattern, characterized by an initial rapid release phase during the first 12 h h, followed by a more controlled release phase. Besides, the amount of released drug in the acidic environment was 2.57-fold higher than in the neutral pH (Cao et al., 2014). Similarly, the current study successfully achieved pH-responsive drug release, comparable to Cao's work, with a more controlled release rate. Recently, Zarrabi and colleagues employed a similar procedure to attach CA to DSPE and PEG2000, forming amide and ester bonds, respectively. They developed a pH-responsive liposome in combination with other phospholipids. Comparable to our study, their release pattern exhibited a controlled and sustained manner, with a greater amount of CUR released at acidic pH compared to neutral pH (Meng et al., 2020). Notably, drug release in our work persisted for a longer time compared to the mentioned study. Our team previously utilized these DSPE-CA-PEG2000 phospholipids to develop a novel smart pH-sensitive niosomal formulation for encapsulating hydrophilic DOX molecules (Saharkhiz et al., 2023).

Here, we employed the previously optimized pH-responsive niosomes to co-encapsulate both hydrophilic DOX and hydrophobic CUR components. We then characterized the resulting particles using various analyses and assessed their bioactivity performances. FTIR results revealed the successful entrapment of both drugs in the carriers, while their simultaneous encapsulation in a particle did not negatively affect the EE% of each other. We hypothesize this may be due to the drugs occupying different spaces within the niosomal particles. Furthermore, SEM images showed uniformly dispersed, round-shaped carriers with an average size of about 200 nm, confirming the DLS outputs. Notably, DOX encapsulation did not affect particle size, while CUR loading between the bilayers resulted in an approximately 30 nm size increase. The release pattern of both drugs followed previously reported literature but exhibited more effective pH responsiveness than other pH-sensitive carriers developed for DOX and CUR co-delivery, such as those by Ghanbari et al. and Zhang and colleagues (Ghanbari et al., 2021; Zhang et al., 2017).

Additionally, we evaluated and compared the therapeutic effect of DOX and CUR co-administration in separate carriers and co-loaded in a single particle on MCF-7 cells. Results demonstrated a synergistic interaction of DOX and CUR in both forms, consistent with the findings of Ghaffari et al. and Sesarman et al. (Sesarman et al., 2019; Ghaffari et al., 2020). However, co-encapsulated form appeared slightly more efficient than the co-administered ones.

It is worth mentioning the possible molecular mechanisms underlying the synergistic effects of DOX and CUR in cancer therapy. Individually, DOX is known to intercalate into DNA, leading to DNA damage, inhibition of topoisomerase II, and ultimately, cell death (Moti et al., 2021). CUR, on the other hand, has been reported to modulate multiple cellular signaling pathways, including NF-κB, PI3K/Akt, and MAPK, leading to the inhibition of proliferation, angiogenesis, and metastasis, as well as the induction of apoptosis in various cancer cells (Hermansyah et al., 2021). In the context of combining DOX with natural compounds, the combination of DOX with genistein, quercetin, or berberine, a natural isoflavone, flavonoid, and alkaloid respectively, demonstrated a synergistic cytotoxic effect in prostate and breast cancer cells through the modulation of PI3K/Akt/mTOR axis and oxidative stress-related

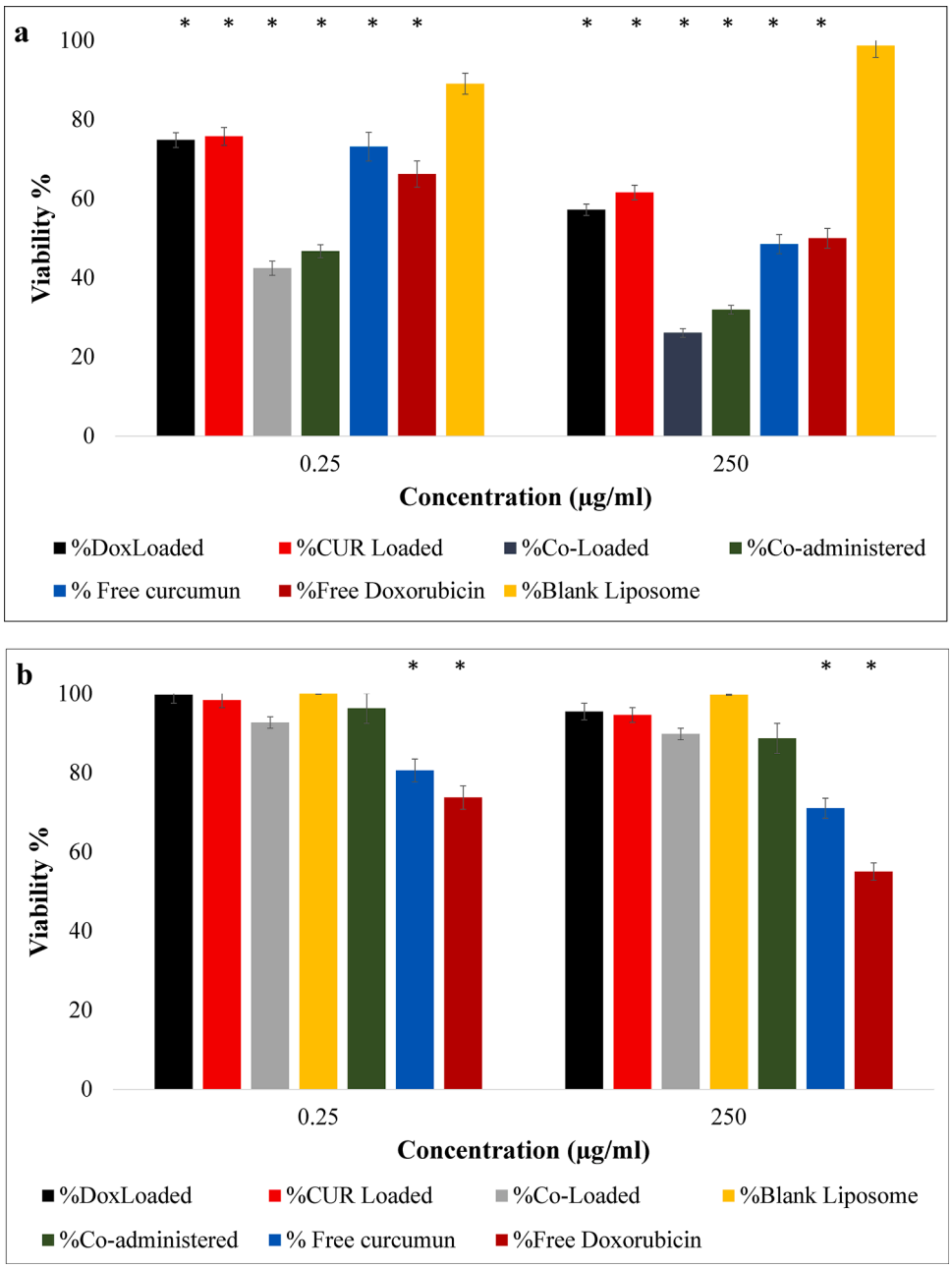

Fig. 5. (a) MTT assay results demonstrating the effects of various treatment forms on MCF-7 breast cancer cells after 72 h h of incubation at 37 °C; (b) MTT assay results for the L929 normal cell line after 72 h h of incubation with different treatment types, highlighting the differential response between cancerous and normal cells. * is an indicator for the significance of each treatment in comparison to the control ($p_{value \leq 0.05}$).

signaling pathways (Hussain et al., 2020; Celik et al., 2022; Wang et al., 2020). Therefore, the synergistic effect of CUR and DOX observed in our study might also involve the modulation of similar signaling pathways, ultimately contributing to enhanced therapeutic efficacy. Despite the good results which were taken from MTT test, it should be considered that this test is not enough to reach to a certain decision in drug development process. Indeed, there are several limitations for measuring the toxicity of a therapeutic material via MTT method including limitations in predictive value (due to its direct relationship with mitochondrial activity, which may not always correlate with cell death or overall drug efficacy) (Van Tonder et al., 2015), inability to capture drug resistance (Stepanenko and Dmitrenko, 2015), lack of immune system interaction (Neufeld et al., 2022), absence of tumor heterogeneity (Van Tonder et al., 2015), etc. Overall, while the MTT assay is a widely used method for assessing drug toxicity in 2D cell cultures, its limitations highlight the need for more physiologically relevant models that better mimic tumor complexity and incorporate factors such as immune system interactions and tumor heterogeneity.

Besides, we used 2D cell culture due to its beneficial effects against 3D culturing such as low cost, user-friendly, simple to set up and maintain, rapid testing of various conditions or compounds and is widely used for the initial screening the effects of therapeutic materials (Kapałczyńska et al., 2018). However, further studies are required to mimic different features of cancerous tissue and elucidate the exact molecular mechanisms underlying the observed synergistic effect.

Regarding the application of pH-responsive vesicular nanoparticles as a drug delivery system, their use is significant, as many of these systems are designed for oral administration and must resist the acidic pH of the stomach. For instance, in year 2020, Leo et al. developed a pH-responsive Eudragit S100 shell that coated curcumin-loaded liposomes

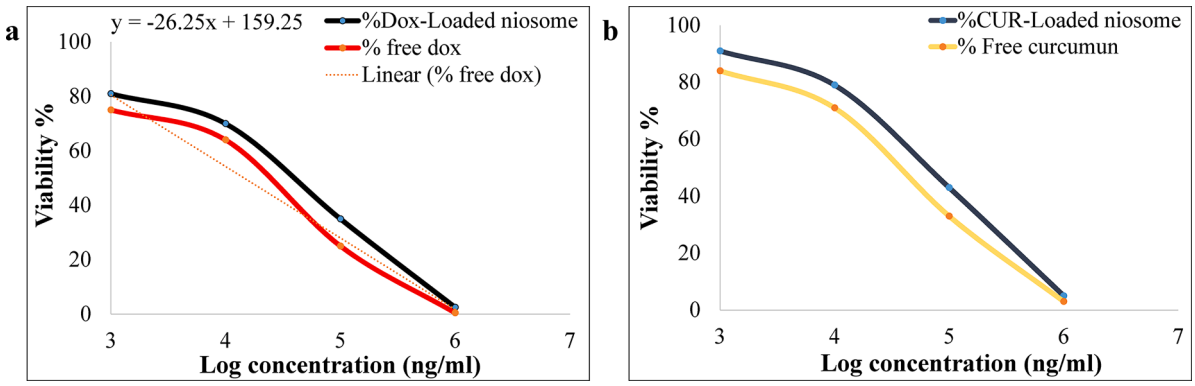

Fig. 6. Inhibition of cell growth in MCF-7 cell line by (a) free DOX and its niosomal form, and (b) free CUR and CUR-loaded niosomes.

Table 6
IC_{50} values of different types of treatments.

Treatment type	IC_{50} values ± SD on MCF-7 cells
Free doxorubicin	129.3 ± 0.21
Free curcumin	138.7 ± 0.32
Free curcumin+Free doxorubicin	50.2 ± 0.14
Dox-loaded niosome	231.2 ± 0.40
Cur-loaded niosome	249.3 ± 0.23
Cur-loaded niosome + Dox-loaded niosome	63.3 ± 0.32
Co-loaded niosome	56.8 ± 0.06

Table 7
CI values of DOX and CUR.

Combination type	CI	Interaction type
Free doxorubicin + Free curcumin	0.66	synergy
DOX-loaded niosome + CUR-loaded niosome	0.88	synergy
DOX and CUR co-loaded niosome	0.71	synergy

CI < 1, synergistic; CI = 1, additive; CI > 1, antagonistic.

for oral administration against colon cancer. These particles protected themselves from the acidic pH of the stomach (De Leo et al., 2020). In contrast, our nano-niosomes are suitable for intravenous injection. These particles significantly increase the solubility and half-life, and reduce the side effects of the therapeutic drug at pH 7.4. Moreover, upon reaching cancerous tissue and in response to the acidic conditions of the tumor tissue, nano-niosomes disintegrate their structure and release their medicinal components exclusively at the targeted site.

5. Conclusions

In summary, our findings demonstrate the successful encapsulation of both DOX and CUR in pH-sensitive niosomal particles. The loading efficiency of these particles was satisfactory, with approximately 77.06 % for DOX and 79.08 % for CUR. The release profile for DOX exhibited an initial burst release followed by a controlled release, while CUR displayed a more sustained release pattern. Furthermore, our experimental results indicated that the co-loading of DOX and CUR in this niosomal formulation led to a synergistic interaction between the therapeutic effect of both drugs and significantly enhanced their cytotoxicity on cancerous cells. This improvement was even more accentuated than when the drugs were co-administrated individually in their respective noisome-encapsulated forms. In conclusion, the co-loading of these two therapeutic agents within the pH-responsive niosome has the potential to increase the efficacy of chemotherapy treatment for patients, while simultaneously reducing the side effects associated with conventional therapies.

CRediT authorship contribution statement

Shaghayegh Saharkhiz: Conceptualization, Methodology, Formal analysis, Investigation, Writing – original draft. **Atefeh Zarepour:** Investigation, Writing – review & editing, Visualization. **Negar Nasri:** Conceptualization, Investigation, Writing – review & editing. **Marco Cordani:** Conceptualization, Investigation, Formal analysis, Writing – review & editing, Visualization, Supervision. **Ali Zarrabi:** Conceptualization, Methodology, Formal analysis, Investigation, Writing – review & editing, Visualization, Supervision.

Declaration of Competing Interest

The authors declare no competing interests.

Data Availability

The datasets generated during and/or analyzed during the current study are available from the corresponding authors on reasonable request.

Acknowledgments

Ali Zarrabi acknowledges funding support from the 1002 - Short Term R&D Funding Program of The Scientific and Technological Research Council of Türkiye (TÜBİTAK, Project No: 221Z107). **Marco Cordani** is supported with a Ramon y Cajal grant (RYC2021–031003-I) from the Spanish Ministry of Science and Innovation, Agencia Estatal de Investigación (MCIN/AEI/10.13039/501100011033), and European UnionNextGeneration (EU/PRTR). **Marco Cordani** acknowledges funding from Spanish Ministry of Universities and Complutense University of Madrid (Maria Zambrano grants for the requalification of the Spanish University System 2021–2023).

References

Abouzeid, A.H., et al., 2013. Anti-cancer activity of anti-GLUT1 antibody-targeted polymeric micelles co-loaded with curcumin and doxorubicin. J. Drug Target. 21 (10), 994–1000.
Aghaei, M., et al., 2021. Non-ionic surfactant vesicles as novel delivery systems for sulfasalazine: evaluation of the physicochemical and cytotoxic properties. J. Mol. Struct. 1230, 129874.
Aibani, N., Khan, T.N., Callan, B., 2020. Liposome mimicking polymersomes; A comparative study of the merits of polymersomes in terms of formulation and stability. Int. J. Pharmaceut.: X 2, 100040.
Aliman, P.T., et al., 2021. Characterization of purified coconut oil bodies as an encapsulating agent for doxorubicin and paclitaxel. Acta Med. Philipp. 55 (4).
Al-Malky, H.S., Al Harthi, S.E., Osman, A.-M.M., 2020. Major obstacles to doxorubicin therapy: cardiotoxicity and drug resistance. J. Oncol. Pharm. Practice 26 (2), 434–444.
Barzegar-Jalali, M., 2008. Kinetic analysis of drug release from nanoparticles. J. pharm. pharmaceut. sci. 11 (1), 167–177.

Cao, J., et al., 2014. Polymeric micelles with citraconic amide as pH-sensitive bond in backbone for anticancer drug delivery. Int. J. Pharm. 471 (1–2), 28–36.
Celik, S., Cakir, E., Akyuz, S., Ozel, A.E., 2022. Flavonoids: their anticarcinogenic effects and molecular modeling studies. Handbook of Research on Natural Products and their Bioactive Compounds as Cancer Therapeutics. IGI Global, pp. 265–296.
Chime, S., Onunkwo, G., Onyishi, I., 2013. Kinetics and mechanisms of drug release from swellable and non swellable matrices: a review. Res. J. Pharm. Biol. Chem. Sci. 4 (2), 97–103.
Chou, T.-C., Motzer, R.J., Tong, Y., Bosl, G.J., 1994. Computerized quantitation of synergism and antagonism of taxol, topotecan, and cisplatin against human teratocarcinoma cell growth: a rational approach to clinical protocol design. JNCI: J. Nat. Cancer Inst. 86 (20), 1517–1524.
Chou, T.-C., Talalay, P., 1984. Quantitative analysis of dose-effect relationships: the combined effects of multiple drugs or enzyme inhibitors. Adv. Enzyme Regul. 22, 27–55.
Dash, S., Murthy, P.N., Nath, L., Chowdhury, P., 2010. Kinetic modeling on drug release from controlled drug delivery systems. Acta Pol. Pharm. 67 (3), 217–223.
De Leo, V., et al., 2020. Eudragit S100 entrapped liposome for curcumin delivery: anti-oxidative effect in Caco-2 cells. Coatings 10 (2), 114.
Dhillon, N., et al., 2008. Phase II trial of curcumin in patients with advanced pancreatic cancer. Clin. cancer res. 14 (14), 4491–4499.
Elfadadny, A., et al., 2023. Natural bioactive compounds-doxorubicin combinations targeting topoisomerase II-alpha: anticancer efficacy and safety. Toxicol. Appl. Pharmacol., 116405
Erfani-Moghadam, V., et al., 2020. ST8 micellar/niosomal vesicular nanoformulation for delivery of naproxen in cancer cells: physicochemical characterization and cytotoxicity evaluation. J. Mol. Struct. 1211, 127867.
Fatima, H., et al., 2023. Chapter 11 - Utility of various drug delivery systems and their advantages and disadvantages. In: Pratap Singh, R., Rb Singh, K., Singh, J., Adetunji, C.O. (Eds.), Nanotechnology for Drug Delivery and Pharmaceuticals. Academic Press, pp. 235–258.
Firouzi Amoodizaj, F., et al., 2020. Enhanced anticancer potency of doxorubicin in combination with curcumin in gastric adenocarcinoma. J. Biochem. Mol. Toxicol. 34 (6), e22486.
Fleege, N.M.G., Cobain, E.F., 2022. Breast Cancer Management in 2021: a Primer for the OB GYN. Best Practice Res. Clin. Obst. Gynaecol.
Foucquier, J., Guedj, M., 2015. Analysis of drug combinations: current methodological landscape. Pharmacol. Res. Perspect. 3 (3), e00149.
Ge, X., Wei, M., He, S., Yuan, W.-E., 2019. Advances of non-ionic surfactant vesicles (niosomes) and their application in drug delivery. Pharmaceutics 11 (2), 55.
Ghaffari, M., et al., 2020. Co-delivery of curcumin and Bcl-2 siRNA by PAMAM dendrimers for enhancement of the therapeutic efficacy in HeLa cancer cells. Colloids Surf. B: Biointerfaces 188, 110762.
Ghanbari, N., et al., 2021. Glucosamine-conjugated graphene quantum dots as versatile and pH-sensitive nanocarriers for enhanced delivery of curcumin targeting to breast cancer. Mater. Sci. Eng.: C 121, 111809.
Gunathilake, T.M.S.U., et al., 2022. Enhanced curcumin loaded nanocellulose: a possible inhalable nanotherapeutic to treat COVID-19. Cellulose 29 (3), 1821–1840.
Guo, W., et al., 2020. Co-delivery of doxorubicin and curcumin with polypeptide nanocarrier for synergistic lymphoma therapy. Sci. Rep. 10 (1), 1–16.
Gupta, S.C., Patchva, S., Aggarwal, B.B., 2013. Therapeutic roles of curcumin: lessons learned from clinical trials. AAPS J. 15, 195–218.
Haghiralsadat, F., et al., 2018. Codelivery of doxorubicin and JIP1 siRNA with novel EphA2-targeted PEGylated cationic nanoliposomes to overcome osteosarcoma multidrug resistance. Int. J. Nanomed. 13, 3853.
Hermansyah, D., et al., 2021. Synergistic effect of Curcuma longa extract in combination with Phyllanthus niruri extract in regulating Annexin A2, epidermal growth factor receptor, matrix metalloproteinases, and pyruvate kinase M1/2 signaling pathway on breast cancer stem cell. Open Access Macedonian J. Med. Sci. 9 (A), 271–285.
Hong, Y., et al., 2019. Lung cancer therapy using doxorubicin and curcumin combination: targeted prodrug based, pH sensitive nanomedicine. Biomed. Pharmacother. 112, 108614.
Hussain, Y., Luqman, S., Meena, A., 2020. Research progress in flavonoids as potential anticancer drug including synergy with other approaches. Curr. Top. Med. Chem. 20 (20), 1791–1809.
Javani, R., Hashemi, F.S., Ghanbarzadeh, B., Hamishehkar, H., 2021. Quercetin-loaded niosomal nanoparticles prepared by the thin-layer hydration method: formulation development, colloidal stability, and structural properties. LWT 141, 110865.
Kapałczyńska, M., et al., 2018. 2D and 3D cell cultures–a comparison of different types of cancer cell cultures. Arch. Med. Sci. 14 (4), 910–919.
Lee, S., Shanti, A., 2021. Effect of exogenous ph on cell growth of breast cancer cells. Int. J. Mol. Sci. 22 (18), 9910.
Liu, D., Yang, F., Xiong, F., Gu, N., 2016. The smart drug delivery system and its clinical potential. Theranostics 6 (9), 1306.
Lookabaugh, B.L., Von Gunten, C.F., et al., 2018. Chapter 34 - approach to the management of cancer pain. In: Benzon, H.T., et al. (Eds.), Essentials of Pain Medicine (Fourth Edition). Elsevier, pp. 299–308 e1.
Meng, W., et al., 2020. Prospects and challenges of extracellular vesicle-based drug delivery system: considering cell source. Drug Deliv. 27 (1), 585–598.
Moti, L.A.A., et al., 2021. Multi-functionalization, a promising adaptation to overcome challenges to clinical translation of nanomedicines as nano-diagnostics and nano-therapeutics for breast cancer. Curr. pharmac. design 27 (43), 4356–4375.
Nematollahi, M.H., et al., 2017. Changes in physical and chemical properties of niosome membrane induced by cholesterol: a promising approach for niosome bilayer intervention. RSC Adv. 7 (78), 49463–49472.
Neufeld, L., Yeini, E., Pozzi, S., Satchi-Fainaro, R., 2022. 3D bioprinted cancer models: from basic biology to drug development. Nature Rev. Cancer 22 (12), 679–692.
Rawat, P.S., et al., 2021. Doxorubicin-induced cardiotoxicity: an update on the molecular mechanism and novel therapeutic strategies for effective management. Biomed. Pharmacother. 139, 111708.
Saharkhiz, S., Zarepour, A., Zarrabi, A., 2023. A new theranostic pH-responsive niosome formulation for Doxorubicin delivery and bio-imaging against breast cancer. Int. J. Pharm., 122845
Sesarman, A., et al., 2018. Anti-angiogenic and anti-inflammatory effects of long-circulating liposomes co-encapsulating curcumin and doxorubicin on C26 murine colon cancer cells. Pharmacol. Rep. 70 (2), 331–339.
Sesarman, A., et al., 2019. Co-delivery of curcumin and doxorubicin in PEGylated liposomes favored the antineoplastic C26 murine colon carcinoma microenvironment. Drug Deliv. Transl. Res. 9, 260–272.
Shehzad, A., Wahid, F., Lee, Y.S., 2010. Curcumin in cancer chemoprevention: molecular targets, pharmacokinetics, bioavailability, and clinical trials. Arch. Pharm. (Weinheim) 343 (9), 489–499.
Stepanenko, A., Dmitrenko, V., 2015. Pitfalls of the MTT assay: direct and off-target effects of inhibitors can result in over/underestimation of cell viability. Gene 574 (2), 193–203.
Tian, Z., et al., 2018. Hyaluronic acid-coated liposome for active targeting on CD44 expressing tumors. J. Nanopart. Res. 20, 1–10.
Van Tonder, A., Joubert, A.M., Cromarty, A.D., 2015. Limitations of the 3-(4, 5-dimethylthiazol-2-yl)-2, 5-diphenyl-2H-tetrazolium bromide (MTT) assay when compared to three commonly used cell enumeration assays. BMC Res. Notes 8, 1–10.
Wang, J., Ma, W., Tu, P., 2015. Synergistically improved anti-tumor efficacy by co-delivery doxorubicin and curcumin polymeric micelles. Macromol. Biosci. 15 (9), 1252–1261.
Wang, Y., et al., 2020. Berberine reverses doxorubicin resistance by inhibiting autophagy through the PTEN/Akt/mTOR signaling pathway in breast cancer. Onco Targets Ther. 13, 1909.
Zarrabi, A., et al., 2021. Synthesis of curcumin loaded smart pH-responsive stealth liposome as a novel nanocarrier for cancer treatment. Fibers 9 (3), 19.
Zarrintaj, P., Saeb, M.R., Jafari, S.H., Mozafari, M., 2020. Application of compatibilized polymer blends in biomedical fields. Compatibilization of Polymer Blends. Elsevier, pp. 511–537.
Zhang, J., et al., 2017. pH-sensitive polymeric nanoparticles for co-delivery of doxorubicin and curcumin to treat cancer via enhanced pro-apoptotic and anti-angiogenic activities. Acta Biomater. 58, 349–364.
Zhang, Q., Wu, L., 2022. In vitro and in vivo cardioprotective effects of curcumin against doxorubicin-induced cardiotoxicity: a systematic review. J. Oncol. 2022.